

High-resolution soil moisture data reveal complex multi-scale spatial variability across the United States

Noemi Vergopolan^{1,2,3*}, Justin Sheffield⁴, Nathaniel W. Chaney⁵, Ming Pan⁶,
Hylke E. Beck⁷, Craig R. Ferguson⁸, Laura Torres-Rojas⁵, Felix Eigenbrod⁴,
Wade Crow⁹, and Eric F. Wood¹

¹Princeton University, Department of Civil and Environmental Engineering, Princeton, NJ, United States

²Princeton University, Atmospheric and Ocean Sciences Program, Princeton, NJ, United States

³NOAA Geophysical Fluid Dynamics Laboratory, Princeton, NJ, United States

⁴University of Southampton, School of Geography and Environmental Sciences, Southampton, United Kingdom

⁵Duke University, Department of Civil and Environmental Engineering, Durham, NC, United States

⁶Center for Western Weather and Water Extremes, Scripps Institution of Oceanography, University of California, CA, United States

⁷European Commission, Joint Research Centre (JRC), Ispra, VA, Italy

⁸University at Albany, State University of New York, Atmospheric Sciences Research Center, Albany, NY, United States

⁹USDA Hydrology and Remote Sensing Laboratory, Beltsville, MD, United States

Key Points:

- 30-m soil moisture (SM) data shows striking and complex spatial variability driven mainly by climate and local variations in soil properties
- This variability yields a remarkable and unique multi-scale behavior at each location that cannot be generalized across the diverse U.S.
- Up to 80% of SM information is lost at the 1-km scale with complete loss at the scale of state-of-the-art SM observation/monitoring systems

*300 Forestal Rd., Atmospheric and Ocean Sciences Program, Sayre Hall, Princeton, NJ, 08544

Corresponding author: Noemi Vergopolan, noemi@princeton.edu

Abstract

Soil moisture (SM) spatiotemporal variability critically influences water resources, agriculture, and climate. However, besides site-specific studies, little is known about how SM varies locally (1–100-m scale). Consequently, quantifying the SM variability and its impact on the Earth system remains a long-standing challenge in hydrology. We reveal the striking variability of local-scale SM across the United States using SMAP-HydroBlocks — a novel satellite-based surface SM dataset at 30-m resolution. Results show how the complex interplay of SM with landscape characteristics and hydroclimate is primarily driven by local variations in soil properties. This local-scale complexity yields a remarkable and unique multi-scale behavior at each location. However, very little of this complexity persists across spatial scales. Experiments reveal that on average 48% and up to 80% of the SM spatial information is lost at the 1-km resolution, with complete loss expected at the scale of current state-of-the-art SM monitoring and modeling systems (1–25 km).

Plain Language Summary

Soil moisture (SM) widely varies in space and time. This variability critically influences freshwater availability, agriculture, ecosystem dynamics, climate and land-atmosphere interactions, and it can also trigger hazards such as droughts, floods, landslides, and aggravate wildfires. Limited SM observational data constrained our understanding of this variability and its impact on the Earth system. Here, we present the first continental assessment of how SM varies at the local scales using SMAP-HydroBlocks – the first 30-m surface SM dataset over the United States. This study maps the SM spatial variability, characterizes the landscape drivers and quantifies how this variability persists across larger spatial scales. Results revealed striking SM spatial variability across the United States, mainly driven by local spatial variations in soil properties and less so by vegetation and topography. However, this SM variability does not persist at coarser spatial scales resulting in extensive information loss. This information loss implicates inaccuracies when predicting non-linear SM-dependent hydrological, ecological, and biogeochemical processes using coarse-scale models and satellite estimates. By mapping the SM spatial variability locally and its scaling behavior, we provide a pathway towards understanding SM-dependent hydrological, biogeochemical, and ecological processes at local (and so far unresolved) spatial scales.

Introduction

Soil moisture (SM) plays a key role in modulating water, energy, and carbon interactions between the land and atmosphere. As such, detailed information is essential for water resources management, natural hazards risk assessment, and understanding ecosystem dynamics, among others. However, SM varies strongly in space, with characteristic length scales ranging from a few centimeters to several kilometers depending on the landscape. SM hotspots that emerge from this spatial variability have significant implications for the scientific understanding and prediction of many hydrological and biogeochemical processes and applications. For instance, SM hotspots influence freshwater sources and agricultural management, as wet and dry conditions require different irrigation and fertilizer interventions for optimal crop growth (Franz et al., 2020; Vergopolan, Xiong, et al., 2021; Sadri et al., 2020). SM spatial variability leads to changes in surface temperature and evapotranspiration (Rouholahnejad Freund et al., 2020), altering drought impacts (Vergopolan, Xiong, et al., 2021) as well as the formation of clouds and convective storms (Simon et al., 2021; Zheng et al., 2021). SM hotspots can alter runoff generation, resulting in faster and peakier flood events (Zhu et al., 2018), and trigger wildfires (Taufik et al., 2017; Holden et al., 2019) and landslides (Wang et al., 2020; Brocca et al., 2016). SM spatial variability influences the distribution of soil fauna and flora, by

75 controlling its habitats, food sources, and dynamics (He et al., 2015; Mathys et al., 2014;
76 Youngquist & Boone, 2014; Sylvain et al., 2014). Depending on landscape characteris-
77 tics (i.e., soils, topography, and vegetation), such SM-driven processes and hazards can
78 occur at local spatial scales (1–100 m). Capturing the SM variability at local scales is
79 critical to further our understanding of these processes and improve our modeling and
80 prediction capabilities.

81 To this end, in-situ SM observations provide detailed information. However, net-
82 works of sensors are costly to deploy and maintain and, therefore, are not widely avail-
83 able over large areas. Microwave-based satellite measurements can provide global SM
84 monitoring with 1–2 days revisit time (Chan et al., 2018; Kerr et al., 2012; Gruber et
85 al., 2019), but retrievals are too coarse (9–36 km) to capture local-scale SM hotspots.
86 Consequently, our current understanding of how SM varies locally is drawn primarily from
87 site-specific studies using in-situ observations (Choi & Jacobs, 2010; Brocca et al., 2007,
88 2012; Crow et al., 2005, 2012; Famiglietti et al., 2008), airborne remote sensing imagery
89 (Famiglietti et al., 2008; Garnaud et al., 2017) and hydrological modeling (Garnaud et
90 al., 2017; Crow et al., 2005), or at larger scales using coarse resolution hydrological mod-
91 eling (Manfreda et al., 2007; Li & Rodell, 2013) or satellite sensors (Das & Mohanty, 2006;
92 Rötzer et al., 2015). These studies have provided a foundational understanding of how
93 hydroclimate and landscape characteristics contribute to SM spatial variability and its
94 underlining mechanisms (Vereecken et al., 2014). They characterize how SM spatial vari-
95 ability is impacted by precipitation (acting as a large-scale driver of runoff (Rosenbaum
96 et al., 2012; Sivapalan et al., 1987)), topography (driving surface and subsurface water
97 flow to the riparian zones; (Famiglietti et al., 2008)), soil properties (controlling soil wa-
98 ter storage, hydraulic conductivity, infiltration, and drying rates (Choi et al., 2007; Crow
99 et al., 2012)), and vegetation (with time-varying physiological functioning influencing
100 soil-water retention, infiltration, and evapotranspiration rates (Joshi & Mohanty, 2010;
101 Mohanty et al., 2000)). However, SM interacts non-linearly with each of these hydro-
102 climate and landscape drivers and as a result the impact of their combined interactions
103 is complex (Vereecken et al., 2014). Because previous local-scale studies tend to be site-
104 specific and with different experiment designs, the transferability of SM spatial variabil-
105 ity across different hydroclimate and diverse landscapes is *unknown*. Consequently, there
106 is no consensus on how SM spatial variability plays out across different hydroclimates
107 and landscapes, and how it influences water, energy, and carbon processes locally. Fur-
108 thermore, little is known about how this variability persists across spatial scales, and whether
109 it can be captured at regional scale by, for example, physical models and microwave satel-
110 lite observations.

111 Here, we present the first characterization of local-scale SM spatial variability at
112 a continental extent and we quantify the persistence of this variability across spatial scales.
113 This assessment was enabled by SMAP-HydroBlocks – a newly developed 30-m satellite-
114 based surface SM dataset for the conterminous United States (CONUS) (Vergopolan,
115 Chaney, et al., 2021a). SMAP-HydroBlocks’ detailed and accurate SM estimates lever-
116 age recent scientific advances in the availability of data from in-situ SM networks, microwave-
117 based satellite remote sensing, gridded meteorological datasets, high-resolution landscape
118 physiography data, and hyper-resolution land surface modeling. As such, SMAP-HydroBlocks
119 provides a unique tool to investigate the SM variability across scales and landscapes, and
120 therefore can help elucidate the role of SM on water, energy, and carbon processes at spa-
121 tial scales that have so far been unresolved (Blöschl et al., 2019). Towards this aim, this
122 work (i) maps the magnitude of SM spatial variability across the CONUS, (ii) quanti-
123 fies the drivers and relationship with hydroclimate and landscape characteristics, and
124 (iii) reveals the multi-scale properties and persistence of this spatial variability across
125 spatial scales. The SM spatial variability is striking in its complexity. We discuss the im-
126 plications of this newly resolved SM variability for quantifying and understanding land-
127 atmosphere interactions and applications in water resources, natural hazard risks, and
128 ecosystem dynamics.

129

The spatial distribution of 30-m soil moisture across the United States

130

131

132

133

134

135

136

137

138

139

140

141

SMAP-HydroBlocks (Vergopolan, Chaney, et al., 2021a) is the first hyper-resolution satellite-based surface SM product at a 30-m resolution over the conterminous United States (2015–2019). It uses a scalable cluster-based merging scheme (Vergopolan et al., 2020) which combines microwave satellite remote sensing, high-resolution land surface model, radiative transfer modeling, machine learning, and in-situ observations to obtain hydrologically consistent SM estimates of the top 5-cm of the soil. SMAP-HydroBlocks was built upon NASA’s Soil Moisture Active Passive L3 Enhanced Global 9-km satellite product (Chan et al., 2018; O’Neill et al., 2019) (SMAP L3E) and HydroBlocks, a field-scale resolving land surface model (Chaney et al., 2021). Validation using independent in-situ observations demonstrated its temporal and spatial representativeness and accuracy, particularly in capturing spatial extremes (Vergopolan, Chaney, et al., 2021a). SMAP-HydroBlocks details are available at Section S1 in the SI.

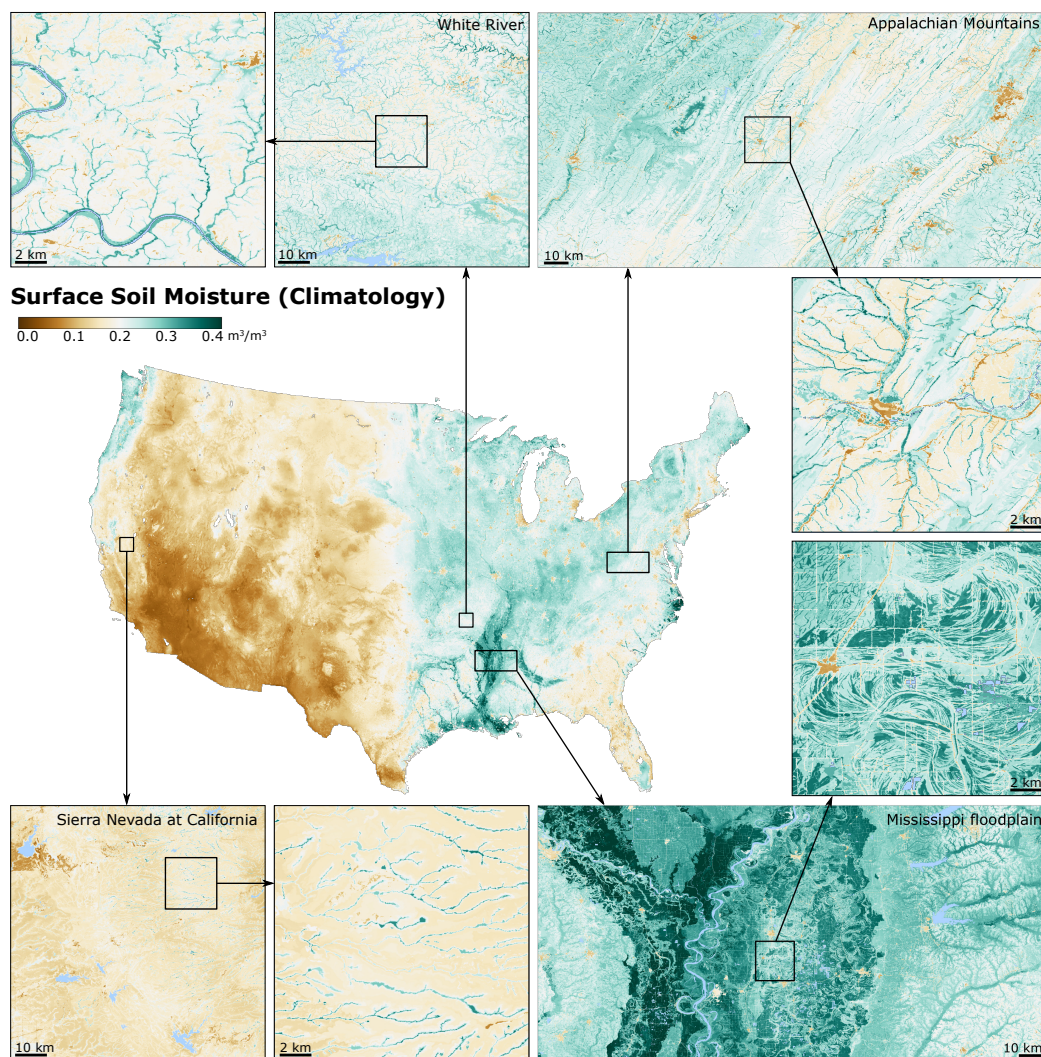


Figure 1. The spatial distribution of surface soil moisture climatology across the CONUS, as shown by the SMAP-HydroBlocks dataset at 30-m spatial resolution (2015–2019). Insets highlight the spatial detail for selected locations with different hydroclimatic and topographical conditions. Water bodies are shown in blue, scale bar is shown at each panel. Interactive visualization of the 30-m data is available at <https://waterai.earth/smaphb>.

142 The SM heterogeneity is demonstrated by SMAP-HydroBlocks substantial spatial
 143 variability from local to continental scales (Fig. 1). At the continental scale, the SM vari-
 144 ability reflects the SM interactions with large-scale hydroclimate and topographic fea-
 145 tures, with distinct drier conditions over the West and Southwest and wetter conditions
 146 over the Midwest, Corn Belt, Mississippi River basin, and Northeast. At the regional and
 147 local scales (Fig. 1 insets), SMAP-HydroBlocks reveals detailed variations that emerge
 148 from the interactions between hydroclimate, topography, soil properties, and land use
 149 heterogeneity across the landscape. In the White River basin and the Appalachian Moun-
 150 tains, for example, we observe the imprint of small tributaries and wet riparian corri-
 151 dors in valleys and wetter conditions over vegetated lowlands. In the Mississippi flood-
 152 plain the topography, historical meandric dunes, and agricultural fields modulate the SM
 153 spatial patterns. Over northern California in the Sierra Nevada, the riparian zone con-
 154 trasts with the dry climate and local aridity.

155 **What is and what drives the spatial variability in soil moisture?**

156 The SM spatial variability across the CONUS is diverse. Here, we quantified using
 157 the spatial standard deviation (σ) – which measures the deviation of local wet and
 158 dry SM hotspots from spatial average conditions over a given domain. We calculated $\sigma_{30\text{ m}}$
 159 using the SMAP-HydroBlocks 30-m SM climatology (2015–2019) at each 10-km box across
 160 the CONUS (details in Section S2 in the SI). Results in Fig. 2a show the largest SM spa-
 161 tial variability in the US Southern Coastal Plain, the lower Mississippi River, and the
 162 Great Lakes region, followed by moderate variability in the Northwestern Pacific, the Ap-
 163 palachian Mountains, and the Northeastern US. The magnitude of this variability is in
 164 agreement with the in-situ observational studies (Vergopolan et al., 2020; Famiglietti et
 165 al., 2008). Regions of high SM variability (shown in orange to red) are linked to wet lo-
 166 cations with substantial precipitation, shallow water table depth (with abundant streams,
 167 ponds, wetlands), variable soil characteristics and verdant vegetation, which can exhibit
 168 significant contrast with respect to their surrounding environment. Low spatial variabil-
 169 ity is seen in most of the US Southwest (typically dry), and at the Northern of the US
 170 Great Plains and the Corn Belt, likely due to flat terrain and cropland dominance that
 171 reduces $\sigma_{30\text{ m}}$.

172 To disentangle the relationships between SM spatial variability with the landscape
 173 and hydroclimate characteristics at each location, we performed a Principal Component
 174 Analysis (PCA) to identify associations with the magnitude of local wet and dry SM hotspots.
 175 In this context, the PCA is particularly useful because it indicates the data dominant
 176 modes of variation (i.e., the principal components) and quantifies how different physi-
 177 cal characteristics co-vary, thus being particularly helpful for identifying strong patterns
 178 in big data. Here, in specific, the PCA compared the SM spatial standard deviation ($\sigma_{30\text{ m}}$,
 179 Fig. 2a) with the spatial mean (μ) and spatial standard deviation (σ) of high-resolution
 180 variables that modulate SM dynamics, such as soil properties (sand, clay, and silt con-
 181 tent), vegetation greenness (e.g., the Normalized Difference Vegetation Index) and land
 182 cover types, elevation and topographic wetness, and climatologies of air temperature and
 183 precipitation at the same 10-km box. Section S3 in the SI details the PCA, the charac-
 184 teristics of these physical drivers, and their spatial distribution (Fig. S1–S5).

185 SM variability tend to follow the dry to wet precipitation gradients (Fig. 2a, Fig.
 186 S5), this pattern is also evident in the PCA (Fig. 2b). Results shows how the SM spa-
 187 tial variability (points) follows the first principal component (PC1), which is dominated
 188 by the precipitation (μ_{precip}) at locations with wetlands and shallow water table depths
 189 (μ_{wetland}), the spatial variability in soil texture (σ_{clay} , σ_{sand}), mean and variability in the
 190 topographic wetness index (μ_{TWI} , σ_{TWI}) while the second component (PC2) is domi-
 191 nated by the soil texture content (μ_{clay} , μ_{sand} , μ_{silt}). In the West coast and most of the
 192 East US, precipitation drives SM spatial variability through the generation of runoff that
 193 is distributed differently across heterogeneous landscapes (Sivapalan et al., 1987) and,

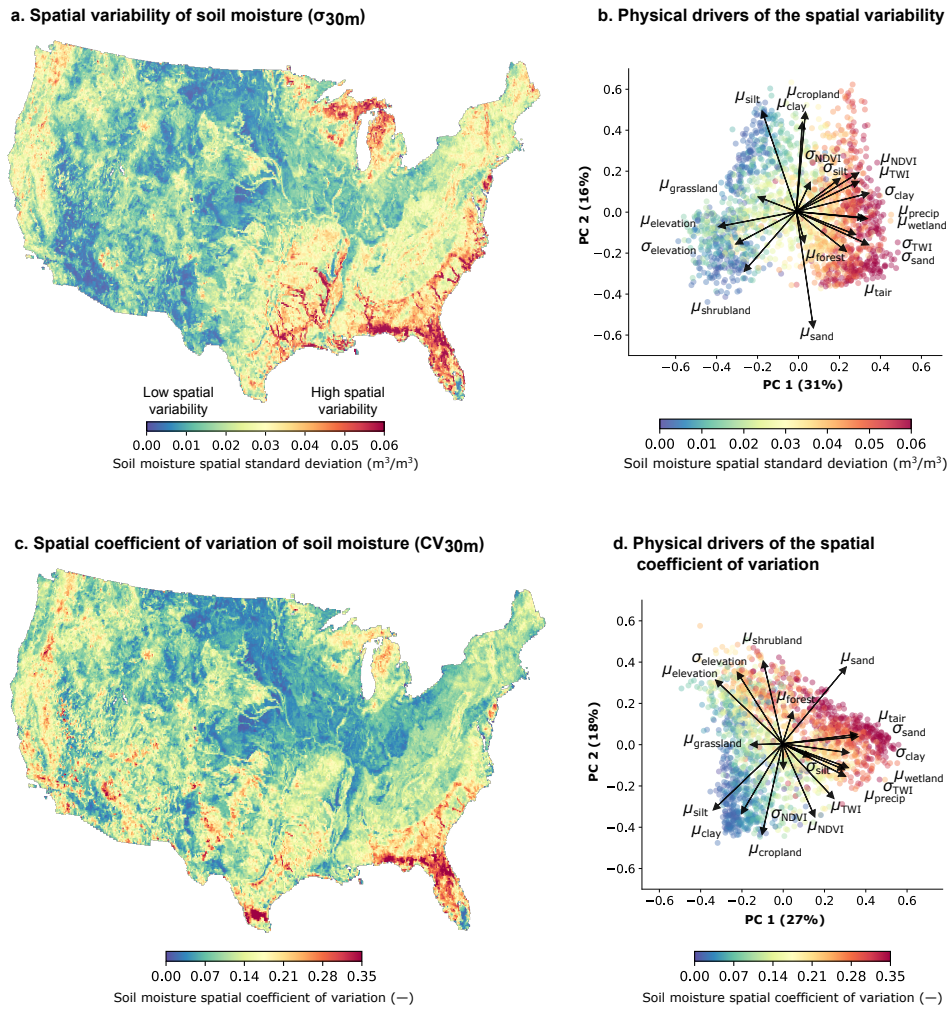


Figure 2. The spatial variability of local-scale soil moisture and its relationship with physical drivers. (a) As a proxy for soil moisture spatial variability, we calculated the spatial standard deviation of the 30-m resolution SMAP-HydroBlocks climatological SM (2015–2019) at each 10-km box across CONUS. Locations in red show where soil moisture spatial variability is highest. (b) The PCA biplot compares the first two components of the relationship between the spatial standard deviation of the 30-m SM (points) with physical characteristics’ spatial mean (μ) and spatial standard deviation (σ) within the same 10-km box (arrows). Similarly, (c) shows the map of the spatial coefficient of variation of SM (as the ratio between spatial standard deviation and the spatial mean), also calculated at each 10-km box, and (d) shows the correspondent PCA biplot. Fig. S1–S5 shows the spatial variation of the physical drivers. Each arrow represents the loading of a physical driver and its direction of variation represents how strongly each driver influences a principal component. The angles between the arrows indicate how the physical characteristics correlate with one another. Arrows pointing towards red (blue) dots show the drivers’ direction of high (low) SM spatial variability.

194 along with the warm temperatures in the South, influences in the long-term the forma-
 195 tion of topographic landscapes and soils through climate and chemical weathering (Breemen
 196 et al., 2002). Soil spatial heterogeneity and variations in its characteristics (e.g., texture,
 197 organic matter content, porosity, and structure) are largely observed in the US south-
 198 east and near the US Great lakes, and drive local variations in soil drying rates, hydraulic
 199 conductivity, and lateral water distribution (Choi et al., 2007; Crow et al., 2012), which
 200 in turn generates more spatially variable SM content. This spatial heterogeneity in soils
 201 (Fig. S1) plays a particular role the SM variability in places with shallow water table
 202 depth, such as the US Southeast, lower and upper Mississippi River valleys (Fig. 1a).
 203 Vegetation characteristics (e.g., type, density, and uniformity) and their changes in time
 204 (i.e., seasonal growth and decay) can dynamically influence SM variability as its phys-
 205 iological functioning and distribution and density of roots can affect soil-water retention,
 206 infiltration, and evapotranspiration rates (Mohanty et al., 2000). Results show high veg-
 207 etation greenness (μ_{NDVI}) and its spatial variability (σ_{NDVI}), correspond to wet locations
 208 of high SM spatial variability (e.g., at the East and West coast). In contrast, in the West
 209 the dry conditions and dominant $\mu_{\text{shrubland}}$ and $\mu_{\text{grassland}}$ types leads to lower SM spa-
 210 tial variability.

211 Topographic characteristics (e.g., surface elevation, slope, topographic wetness in-
 212 dex, aspect, and curvature) drive SM convergence to riparian zones via surface and sub-
 213 surface lateral flow (Crow et al., 2012). Results show high SM variability linked to high
 214 topographic wetness index (μ_{TWI}) and its spatial variability (σ_{TWI}), demonstrating the
 215 role of topography in driving SM spatial patterns, particularly at the US Southeast coast,
 216 lower and upper Mississippi basins. However, topographic control on surface SM tends
 217 to happen mostly during and after rainfall events (Western et al., 2003). In contrast, dur-
 218 ing drydown and typical conditions, the influence of soil properties and vegetation will
 219 dominate (Chang & Islam, 2003; Ryu & Famiglietti, 2005). In fact, the results also show
 220 locations of high elevation ($\mu_{\text{elevation}}$) and spatially variable topography ($\sigma_{\text{elevation}}$), as
 221 in most of the US West, linked to low SM spatial variability (Fig. 2b) because most of
 222 the locations of high elevation gradients in the West tend to be climatologically drier (Fig.
 223 S6). In contrast, at climatologically wet locations, such as over the Appalachian moun-
 224 tains (Fig. 2a and Fig. 1), substantial SM spatial variability is shown. SM spatial vari-
 225 ability is known to be higher at wetter soils (Famiglietti et al., 2008). To isolate the con-
 226 tribution of other physical drivers from the influence of dry/wet conditions, we computed
 227 the SM spatial coefficient of variation ($CV_{30\text{m}}$), which represents the SM spatial vari-
 228 ability normalized by the soil wetness (Fig. 2c). The PCA of $CV_{30\text{m}}$ (Fig. 2d) shows that
 229 spatial variability in soil texture (σ_{clay} , σ_{sand}) still dominates with the SM variability,
 230 followed by air temperature (μ_{tair}) and sand content (μ_{sand}). This is particularly evi-
 231 dent over the US Southeast where high spatially variable and quick drying sandy soils
 232 at the surface interact with a low water table depth and wetlands and results in distinct
 233 wet and dry SM hotspots. Fig. 2d also shows the topographic drivers ($\mu_{\text{elevation}}$, $\sigma_{\text{elevation}}$,
 234 μ_{TWI} , and σ_{TWI}), vegetation characteristics (μ_{NDVI} , σ_{NDVI} , $\mu_{\text{shrubland}}$, μ_{forest}), and pre-
 235 cipitation (μ_{precip}) shifted towards PC2, highlighting their secondary role in driving the
 236 SM $CV_{30\text{m}}$. As shown here, the strength of SM hotspots and their local spatial variabil-
 237 ity emerges from the combined and non-linear hydrological processes and their interac-
 238 tions with climatic conditions, topography, soils, and vegetation dynamics. However, at
 239 each location, different characteristics and physical processes will contribute differently
 240 and lead to patterns that cannot be generalized by the independent contribution of a few
 241 key drivers.

242 **Where and how does soil moisture variability persists across spatial** 243 **scales?**

244 Depending on the landscape complexity, the SM spatial variability at the local scale
 245 may not persist at regional scales and therefore cannot be represented by coarse reso-

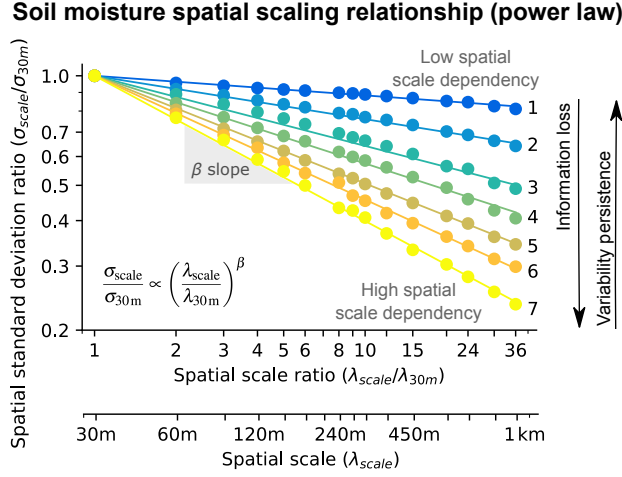


Figure 3. The scaling of soil moisture spatial variability. Illustration shows how soil spatial scaling follows a power-law relationship. The graph compares the soil moisture spatial standard deviation ratio of data at a coarse spatial scale with respect to the 30-m data ($\sigma_{\text{scale}}/\sigma_{30\text{m}}$). As the spatial scale increases (decreasing spatial resolution), the spatial standard deviation ratio decreases. The decrease in spatial variability follows a power-law relationship. β quantifies the strength of the inverse relationship between data scale and spatial variability. The larger the β slope, the larger is the spatial-scale dependency, meaning that the SM spatial variability does not persist and there is a larger information loss at coarser spatial scales. We selected seven locations across the CONUS (shown in Fig. 4b) that illustrate a range of different scaling behaviors (lines).

246 lution data (e.g., from models or microwave satellite observations). The inability to rep-
 247 resent this variability dampens the strength of local SM hotspots and could hamper the
 248 utility of SM information for water resources management and understanding of land-
 249 atmosphere interactions at local scales. In fact, quantifying how SM spatial variability
 250 changes across scales and its impact on the Earth system remains a critical unsolved prob-
 251 lem in hydrology (Blöschl et al., 2019; Crow et al., 2012). Here, we characterize the scal-
 252 ing properties of SM spatial variability by mapping how this variability changes across
 253 spatial scales and where it persists. This also helps to identify where high-resolution data
 254 is critical to capture local-scale variability.

255 To this end, we performed a synthetic spatial scaling analysis, which involves up-
 256 scaling the 30-m SMAP-HydroBlocks data to coarser spatial scales (λ_{scale} : 60 m, 90 m,
 257 ..., 1 km) and calculating the change in spatial standard deviation (i.e., change in vari-
 258 ability) at each scale with respect to the 30-m data ($\sigma_{\text{scale}}/\sigma_{30\text{m}}$). Observational stud-
 259 ies at a few sites have shown that this change in SM spatial variability with data sup-
 260 porting scale and spacing follows a power-law relationship (Rodriguez-Iturbe et al., 1995).
 261 This behavior turned out to be the same observed when comparing SM correlation length
 262 and distance, and it often characterizes complex hydrological fractal nature (Famiglietti
 263 et al., 2008). As illustrated in Fig. 3, the log relationship between the spatial standard
 264 deviation ratio and data scale indicates the strength of the SM spatial scale dependency
 265 through β , and it can be interpreted as an indicator of SM variability persistence across
 266 scales (Hu et al., 1997). The more negative the β , the larger is the dependency of the
 267 SM spatial variability on the data scale. Consequently, higher information loss (herein
 268 defined as $1 - \sigma_{\text{scale}}/\sigma_{30\text{m}}$) and lower variability persistence are expected at coarser spa-
 269 tial resolutions. Although SM spatial patterns can change over time, its spatial signa-

270 ture persists (Mälicke et al., 2020). As a result, β does not change significantly over time
 271 (e.g., during SM drydown) making it a stable metric for characterizing multi-scaling SM
 272 properties (Oldak et al., 2002).

273 The scaling relationship for selected sites of varying landscape complexity are il-
 274 lustrate in Fig. 3 and 4a. The small β value of -0.06 (Location 1, Fig. 3) indicates lit-
 275 tle change in spatial standard deviation with scale and persistence of local-scale SM hotspots
 276 across scales. At 1-km resolution, only 21% of the spatial variability is lost with respect
 277 to the 30-m data (Fig. 4a, first row). In contrast, the scaling relationship at Location
 278 7 shows a large β (-0.37) associated with a 74% reduction in spatial variability. In fact,
 279 the imprint of the riparian zone within this site vanishes at 1-km resolution (Fig. 4a last
 280 row), exemplifying the high spatial scale dependency and lack of spatial variability per-
 281 sistence. Fig. 4b maps the information loss (as a percentage) when the 30-m SM data
 282 is averaged to 1-km resolution (Fig. S7 maps the β coefficient) across CONUS. Over-
 283 all, there is little persistence of SM spatial variability across scales, with an average in-
 284 formation loss of $48 \pm 10\%$, and a maximum loss of 80%. Importantly, this information
 285 loss (and the associated β) strongly varies by location, revealing complex context-dependent
 286 multi-scale properties (Fig. 4b). A PCA in Fig. 4d compares the strength of this infor-
 287 mation loss with the mean and spatial variability of landscape and climate character-
 288 istics. Results showed a tendency for high information loss at locations with strong to-
 289 pographic gradients (such as over the Rocky Mountains, Appalachian Mountains, North-
 290 western Cascade Range, and the Sierra Nevada) and dominant forest coverage (e.g., most
 291 of the Northeast). However, for information loss below 60% the results shows no clear
 292 or generalizable relationship with climatic and physiographic characteristics. We also com-
 293 pared the relationship between information loss and SM spatial standard deviation (Fig.
 294 5a). High and low information loss can emerge from either high or low SM spatial vari-
 295 ability, but with zero correlation. This demonstrates how the complex and non-linear
 296 hydrological, ecohydrological, and biogeochemical processes that occur at local scales yield
 297 such unique SM scaling behavior locally that can hardly be transferred to different hy-
 298 droclimates and landscapes.

299 Mapping where SM spatial variability and information loss are highest is critical
 300 to identify where high-resolution data is needed. Fig. 5b shows low SM spatial variabil-
 301 ity with high information loss (dark blue) in most of the US Corn Belt and the Missouri
 302 River basin, driven mainly by cropland dominance and flat terrain. These small-scale
 303 variations vanish at the 1-km resolution but are critical to capturing intra-field scale ir-
 304 rigation water demands (Franz et al., 2020). Low variability with high information loss
 305 is also observed in parts of the Rocky Mountains and the West, where dry conditions lead
 306 to low SM variability. However, topographic gradients enhance information loss, ham-
 307 pering the monitoring of (already scarce) freshwater resources. High SM variability and
 308 information loss (dark orange) are present on the US West coast (e.g., Sierras Nevada
 309 and the Cascade Range) and most of the Northeastern US (including the Appalachians),
 310 driven by precipitation interactions with topography that replenishes the riparian zones.
 311 High SM variability and information loss are also evident near the US Great Lakes, lower
 312 Mississippi River, and the Southeast coast, driven by heterogeneity in soils driving spa-
 313 tially variable SM dry-down rates contrasting with wetlands and shallow water table depths.
 314 Given the high SM variability and information loss, further allocating in-situ monitor-
 315 ing resources at locations is thus critical for better monitoring and quantifying non-linear
 316 SM-dependent hydrological, ecological, and biogeochemical processes.

317 **Implications**

318 **Understanding and modeling land-atmosphere feedbacks**

319 Studies have shown how neglecting the SM spatial variability at local scales damp-
 320 ens extremes and introduces errors when quantifying scale-dependent water, energy, and

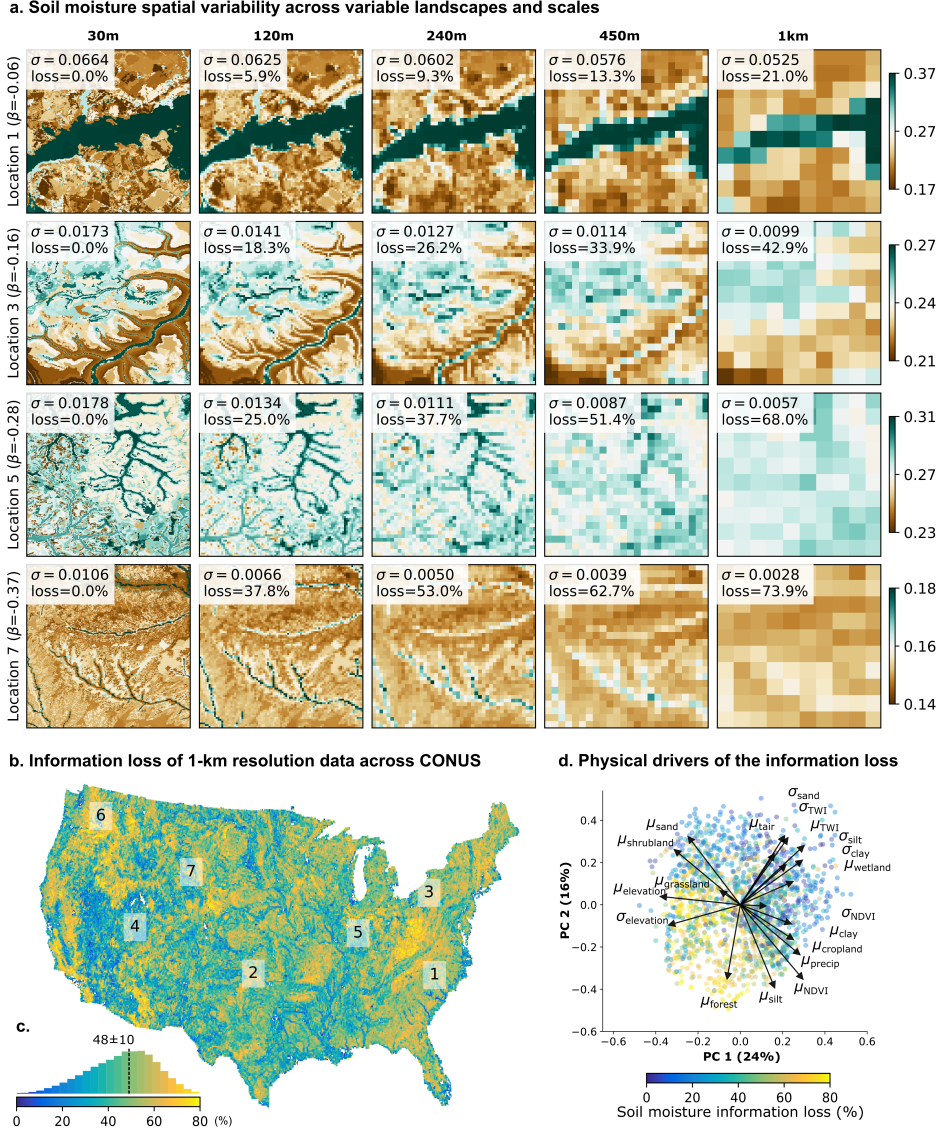


Figure 4. The information loss of soil moisture across spatial scales. (a) Comparison of the soil moisture data at different spatial resolutions: each panel shows SM at a 10-km box with its climatological spatial variability (measured by the spatial standard deviation, σ), and information loss (measured as the percentage change in spatial standard deviation with respect to the 30-m data). Each row shows a different location (subsampled from the 7 locations in Fig. 3) and each column shows data at different resolutions. (b) We mapped the information loss of the 1-km resolution data for each 10-km box across the CONUS. Locations in orange to yellow show where coarser spatial resolution data fail to capture 60–80% of the spatial variability observed at 30-m resolution. Subplot (c) shows the distribution of this information loss in the US. (d) PCA biplot compares the first two components of the relationship between the information loss (points) with physical characteristics’ spatial mean (μ) and spatial standard deviation (σ) within the same 10-km boxes (arrows). Fig. S1–S5 shows the spatial variation of the physical drivers. Each arrow represents the loading of a physical driver and its direction of variation represents how strongly each driver influences a principal component. The angles between the arrows indicate how the physical characteristics correlate with one another. Arrows pointing towards yellow (blue) dots show the drivers’ direction of high (low) soil moisture information loss.

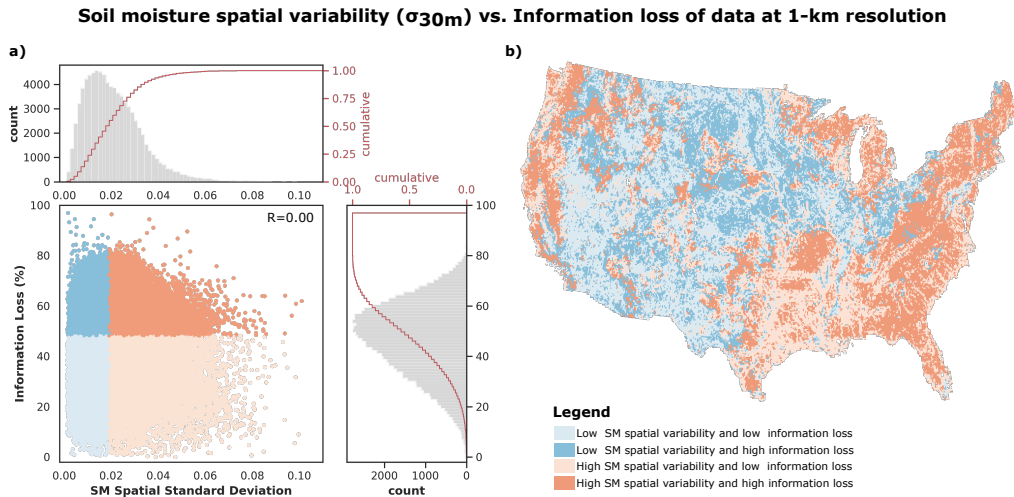


Figure 5. Comparison between the spatial variability of SM data at 30-m resolution and information loss of the 1-km resolution SM data. Panel a) compares the joint distribution of the SM spatial standard deviation (x-axis) and the information loss (y-axis) of all 10-km boxes across CONUS. To identify locations with low or high SM spatial variability and information loss, the data space was partitioned in 4 domains, based on the average SM spatial standard deviation (0.02) and average information loss (48%). Adjacent top and lateral graphs show the histograms and cumulative functions of the SM spatial standard deviation and information loss, respectively. Panel b) maps each of the 4 domains with the same color scheme: blue (orange) colors show areas of low (high) SM spatial variability, whereas light (dark) colors show areas of low (high) information loss. In panel b, orange colors emphasize the high SM variability patterns (observed in Fig. 2a), while the dark (blue and orange) colors emphasize the high information loss patterns (observed in Fig. 4b).

321 carbon interactions between the land and the atmosphere. For example, the relationship
 322 between SM and evapotranspiration under different water and energy constraints is highly
 323 non-linear (Rouholahnejad Freund & Kirchner, 2017). When wet SM hotspots are re-
 324 solved at spatial scales closer to their true spatial variability, they enhance evapotran-
 325 spiration to the atmosphere in comparison to spatially homogeneous drier conditions (Crow
 326 & Wood, 2002; Rouholahnejad Freund et al., 2020). This higher evapotranspiration fur-
 327 ther cools the ground surface, and can enhance horizontal atmospheric humidity and tem-
 328 perature gradients that drive variable boundary layer dynamics, development of large-
 329 scale eddies, potentially triggering of local convective rainfall (Simon et al., 2021; Ford
 330 et al., 2015; Zheng et al., 2021; Vergopolan & Fisher, 2016). Spatially variable SM also
 331 controls plant photosynthesis rates and nutrient cycling, yielding non-linear changes of
 332 40–80% in carbon uptake (Trugman et al., 2018; Green et al., 2019) and 78% nitrogen
 333 cycling (Paul et al., 2003). For instance, optimal crop nitrogen uptake is inhibited by
 334 both very dry and wet SM conditions. While dry SM inhibits mineralization, extreme
 335 wet SM lead to denitrification and N_2O release (Paul et al., 2003) — a greenhouse gas
 336 298 times more effective at trapping heat in the atmosphere than CO_2 (Denman et al.,
 337 2007). As such, the spatial variability in SM critically changes the flux response of highly
 338 non-linear and local-scale processes, while grid-average conditions can lead to inaccurate
 339 assessment and process interpretation. Limited observations have historically constrained
 340 understanding of the impact of SM variability on these processes. The spatial variabil-
 341 ity of SMAP-HydroBlocks allows quantifying these processes’ dependencies and iden-
 342 tifying where fine-scale data is critical for improving our understanding of the land-atmosphere

343 and biogeochemical processes that drive changes in weather and climate and our abil-
344 ity to model them.

345 **Supporting water resources decision-making and natural hazards risks**

346 Local scale SM spatial variability also impacts management of freshwater resources
347 and water-dependent risks. For instance, when local dry or wet SM hotspots are aver-
348 aged by coarse-resolution SM data, the perceived intensity of drought conditions or ex-
349 tent of waterlogging is reduced. The related underestimation (or overestimation) of crop
350 water demands limits farmer decision making on when and where to irrigate (Franz et
351 al., 2020; Vergopolan, Xiong, et al., 2021). Capturing SM dynamics at the field scale is
352 thus critical to quantify irrigation (Jalilvand et al., 2019; Dari et al., 2020). SM spatial
353 variability also impacts on wildfires by controlling the spatial distribution of vegetation
354 fuel load and flammability through vegetation water content (Taufik et al., 2017; O et
355 al., 2020). As such, the inability to represent wet and dry SM hotspots at sub-kilometer
356 scales results in underestimated risks of propagating wildfires (Holden et al., 2019). Sim-
357 ilarly, local wet hotspots lead to conditions that trigger landslides and local flash floods.
358 Landslides tends to happen at small-scale (e.g., $\sim 10\text{--}100\text{-m}^2$, Zhang et al. (2019)) and
359 occur when soil water saturation increases soil-column weight, reduces soil cohesion, and
360 leads to gravity-driven mass movements. Wet hotspots that trigger these events are mostly
361 averaged out by coarser-resolution data, critically limiting monitoring of slope stability
362 and landslide detection accuracy (Wang et al., 2020). Spatially variable SM also drives
363 spatial variability rainfall infiltration rates which influence the timing and spatial struc-
364 ture of runoff generation and flooding, leading to earlier and more intense floods (Zhu
365 et al., 2018).

366 **Monitoring and understanding biodiversity and species distribution**

367 SM spatial variability plays a critical role in controlling land ecosystems (Rodríguez-
368 Iturbe & Porporato, 2007), particularly soil organisms and communities (Sylvain et al.,
369 2014; Mathys et al., 2014), but also amphibian movements (Youngquist & Boone, 2014),
370 and species distributions more generally (Gardner et al., 2019). Soil organisms that are
371 closely coupled with SM are especially important as they comprise 25–33% of Earth’s
372 biodiversity (Decaëns et al., 2006), providing vital ecosystem functions such as soil fer-
373 tilization, nutrient recycling, pest and disease regulation, and erosion (Qiu & Turner, 2015;
374 Wall, 2013). Variability in SM leads to patchy and reduced distribution of suitable habi-
375 tats for such soil organisms and influence their dynamics (Wall & Virginia, 1999). Par-
376 ticularly in arid and degraded conditions, this leads to reduced local biodiversity and ecosys-
377 tem function and to increased susceptibility to disturbances (Wall & Virginia, 1999). There-
378 fore, characterization of SM spatial variability and information loss provide insights on
379 organisms’ dynamics, behavior, biodiversity richness, and ecosystem service provision
380 (He et al., 2015). SM also plays a critical role in determining the degree of drought stress
381 of plants (Vergopolan, Xiong, et al., 2021); a failure to account for local variability can
382 lead to underestimates of the effects of climate change on future distributions (Midgley
383 et al., 2002). In addition, SM play a key role in enabling detailed monitoring of pest in-
384 festation food sources and reproduction pathways (Gómez et al., 2020), and supporting
385 the assessment and forecasting of infectious disease and pest risks such as West Nile virus,
386 malaria, and locust swarms (Keyel et al., 2019; Escorihuela et al., 2018). Understand-
387 ing SM variability and scaling at the local scale is therefore critical for improving un-
388 derstanding and monitoring of ecosystems dynamics, pest infestations, and biodiversity
389 loss in a spatially explicit manner. Furthermore, it supports the development of adap-
390 tation pathways towards improving these ecosystems’ resilience to climate variability and
391 climate change.

Conclusion

Understanding SM spatial variability, its scaling behavior, and effects on freshwater resources is a long-standing grand challenge in hydrology. By mapping SM variability at unprecedented scales, our study reveals the unseen and striking local-scale variability across CONUS. The magnitude of this variability and information loss across scales varies widely across landscapes, highlighting how SM-dependent water, energy, and carbon processes cannot be reduced to simplistic relations with hydroclimate or landscape characteristics. Yet, this local-scale complexity demonstrated by SMAP-HydroBlocks is not represented by current SM monitoring and modeling systems (1–25-km resolution) and hinders our ability to address a range of scientific questions and applications on land-atmosphere feedbacks, water resources management, and biodiversity and species distributions. The SM variability and information loss mapped here can critically aid resources allocation and design of in-situ networks for improved monitoring of non-linear and SM-dependent hydrological, biogeochemical and ecological processes. Given recent advances in data availability and computing resources, the next generation of SM products, land surface models, and Earth system models should also consider how to account for this local scale variability to more realistically represent hydrological processes, natural hazards, and its interactions with climate. By mapping the SM variability and its scaling behavior, this work provides a pathway towards improving the understanding and quantification of hydrological, biogeochemical, and ecological processes at spatial scales that have so far been unresolved.

Data Availability

The SMAP-HydroBlocks surface soil moisture dataset at 30-m 6-h resolution (2015–2019) comprises a 62 TB dataset (with maximum compression). Due to the storage limitation of online repositories, we provide the raw data at the Hydrologic Response Unit (HRU) level (time, hru) compressed to 33 GB. Python code and instructions for post-processing the data into geographic coordinates (time, latitude, longitude) is available at GitHub (https://github.com/NoemiVergopolan/SMAP-HydroBlocks_postprocessing). Data are available for download at Vergopolan et al. (Vergopolan, Chaney, et al., 2021b) (<https://doi.org/10.5281/zenodo.5206725>). The data are provided in netCDF-4 format (<https://www.unidata.ucar.edu/software/netcdf/>), and referenced to the World Geodetic Reference System 1984 (WGS 84) ellipsoid. The netCDF-4 files can be viewed, edited, and analyzed using most Geographic Information Systems (GIS) software packages, including ArcGIS, QGIS, and GRASS. As an illustration example, a 30-m map of the SMAP-HydroBlocks annual and long-term climatology can be viewed through an interactive web interface at <https://waterai.earth/smaphb>.

Acknowledgments

This work was supported by the “Modernizing Observation Operator and Error Assessment for Assimilating In-situ and Remotely Sensed Snow/Soil Moisture Measurements into NWM” project from NOAA (grant number NA19OAR4590199), the “Understanding Changes in High Mountain Asia project” project from NASA (grant number NNH19ZDA001N-HMA), the NASA-NOAA Interagency Agreement through the High Mountain Asia program (grant number 80HQTR21T0015), the “A new paradigm in precision agriculture: assimilation of ultra-fine resolution data into a crop-yield forecasting model” project from the King Abdullah University of Science and Technology (grant number OSR-2017-CRG6), and the “Building REsearch Capacity for sustainable water and food security In drylands of sub-saharan Africa (BREC-cIA)” project from the UK Research and Innovation as part of the Global Challenges Research Fund (grant number NE/P021093/1).

References

440

- 441 Blöschl, G., Bierkens, M. F., Chambel, A., Cudennec, C., Destouni, G., Fiori, A.,
 442 ... van Oel, P. R. (2019, 07). Twenty-three unsolved problems in hydrology
 443 (uph) – a community perspective. *Hydrological Sciences Journal*, 1-18. doi:
 444 <https://doi.org/10.1080/02626667.2019.1620507>
- 445 Breemen, N. V., Buurman, P., & Ebrary, I. (2002). *Soil formation*. Kluwer Aca-
 446 demic.
- 447 Brocca, L., Ciabatta, L., Moramarco, T., Ponziani, F., Berni, N., & Wagner, W.
 448 (2016). Use of satellite soil moisture products for the operational mitigation of
 449 landslides risk in central italy. *Satellite Soil Moisture Retrieval*, 231-247. doi:
 450 <https://doi.org/10.1016/b978-0-12-803388-3.00012-7>
- 451 Brocca, L., Morbidelli, R., Melone, F., & Moramarco, T. (2007, 02). Soil moisture
 452 spatial variability in experimental areas of central italy. *Journal of Hydrology*,
 453 333, 356-373. doi: <https://doi.org/10.1016/j.jhydrol.2006.09.004>
- 454 Brocca, L., Tullo, T., Melone, F., Moramarco, T., & Morbidelli, R. (2012, 02).
 455 Catchment scale soil moisture spatial-temporal variability. *Journal of Hydrol-
 456 ogy*, 422-423, 63-75. doi: <https://doi.org/10.1016/j.jhydrol.2011.12.039>
- 457 Chan, S., Bindlish, R., O'Neill, P., Jackson, T., Njoku, E., Dunbar, S., ... Kerr,
 458 Y. (2018, 01). Development and assessment of the smap enhanced passive
 459 soil moisture product. *Remote Sensing of Environment*, 204, 931-941. doi:
 460 <https://doi.org/10.1016/j.rse.2017.08.025>
- 461 Chaney, N. W., Metcalfe, P., & Wood, E. F. (2016, 08). Hydroblocks: a field-scale
 462 resolving land surface model for application over continental extents. *Hydrolog-
 463 ical Processes*, 30, 3543-3559. doi: <https://doi.org/10.1002/hyp.10891>
- 464 Chaney, N. W., Minasny, B., Herman, J. D., Nauman, T. W., Brungard, C. W.,
 465 Morgan, C. L. S., ... Yimam, Y. (2019, 04). Polaris soil properties: 30-
 466 m probabilistic maps of soil properties over the contiguous united states.
 467 *Water Resources Research*, 55, 2916-2938. doi: <https://doi.org/10.1029/2018wr022797>
- 468
- 469 Chaney, N. W., Torres-Rojas, L., Vergopolan, N., & Fisher, C. K. (2021). Hy-
 470 droblocks v0.2: enabling a field-scale two-way coupling between the land
 471 surface and river networks in earth system models. *Geoscientific Model Devel-
 472 opment*, 14(11), 6813-6832. Retrieved from [https://gmd.copernicus.org/](https://gmd.copernicus.org/articles/14/6813/2021/)
 473 [articles/14/6813/2021/](https://doi.org/10.5194/gmd-14-6813-2021) doi: <https://doi.org/10.5194/gmd-14-6813-2021>
- 474 Chang, D. H., & Islam, S. (2003). Effects of topography, soil properties and mean
 475 soil moisture on the spatial distribution of soil moisture: A stochastic analysis.
 476 In (p. 193 – 225). CRC Press.
- 477 Choi, M., & Jacobs, J. M. (2010, 09). Spatial soil moisture scaling structure dur-
 478 ing soil moisture experiment 2005. *Hydrological Processes*, 25, 926-932. doi:
 479 <https://doi.org/10.1002/hyp.7877>
- 480 Choi, M., Jacobs, J. M., & Cosh, M. H. (2007, 01). Scaled spatial variability of soil
 481 moisture fields. *Geophysical Research Letters*, 34. doi: [https://doi.org/10](https://doi.org/10.1029/2006gl028247)
 482 [.1029/2006gl028247](https://doi.org/10.1029/2006gl028247)
- 483 Crow, W. T., Berg, A. A., Cosh, M. H., Loew, A., Mohanty, B. P., Panciera, R., ...
 484 Walker, J. P. (2012, 04). Upscaling sparse ground-based soil moisture obser-
 485 vations for the validation of coarse-resolution satellite soil moisture products.
 486 *Reviews of Geophysics*, 50. doi: <https://doi.org/10.1029/2011rg000372>
- 487 Crow, W. T., Ryu, D., & Famiglietti, J. S. (2005, 01). Upscaling of field-scale soil
 488 moisture measurements using distributed land surface modeling. *Advances in
 489 Water Resources*, 28, 1-14. doi: [https://doi.org/10.1016/j.advwatres.2004.10](https://doi.org/10.1016/j.advwatres.2004.10.004)
 490 [.004](https://doi.org/10.1016/j.advwatres.2004.10.004)
- 491 Crow, W. T., & Wood, E. F. (2002, 08). The value of coarse-scale soil moisture ob-
 492 servations for regional surface energy balance modeling. *Journal of Hydromete-
 493 orology*, 3, 467-482. doi: [https://doi.org/10.1175/1525-7541\(2002\)003<0467:](https://doi.org/10.1175/1525-7541(2002)003<0467:tvocss>2.0.co;2)
 494 [tvocss\)2.0.co;2](https://doi.org/10.1175/1525-7541(2002)003<0467:tvocss>2.0.co;2)

- 495 Danielson, J. J., & Gesch, D. B. (2011). *Global multi-resolution terrain elevation*
 496 *data 2010 (gmted2010)*. US Department of the Interior, US Geological Survey.
- 497 Dari, J., Brocca, L., Quintana-Seguí, P., Escorihuela, M. J., Stefan, V., & Morbidelli,
 498 R. (2020, 08). Exploiting high-resolution remote sensing soil moisture to esti-
 499 mate irrigation water amounts over a mediterranean region. *Remote Sensing*,
 500 *12*, 2593. doi: 10.3390/rs12162593
- 501 Das, N. N., & Mohanty, B. P. (2006). Root zone soil moisture assessment using re-
 502 mote sensing and vadose zone modeling. *Vadose Zone Journal*, *5*, 296. doi:
 503 <https://doi.org/10.2136/vzj2005.0033>
- 504 Decaëns, T., Jiménez, J., Gioia, C., Measey, G., & Lavelle, P. (2006, 11). The values
 505 of soil animals for conservation biology. *European Journal of Soil Biology*, *42*,
 506 S23-S38. doi: <https://10.1016/j.ejsobi.2006.07.001>
- 507 Denman, K. L., Brasseur, G., Chidthaisong, A., Ciais, P., Cox, P. M., Dickinson,
 508 R. E., ... Jacob, D. (2007). Couplings between changes in the climate system
 509 and biogeochemistry. In (p. 499–588). Cambridge University Press.
- 510 Escorihuela, M. J., Merlin, O., Stefan, V., Moyano, G., Eweys, O. A., Zribi, M.,
 511 ... Piou, C. (2018, 08). Smos based high resolution soil moisture estimates
 512 for desert locust preventive management. *Remote Sensing Applications: So-*
 513 *ciety and Environment*, *11*, 140-150. Retrieved 2019-11-05, from [https://](https://www.sciencedirect.com/science/article/pii/S2352938517302392)
 514 www.sciencedirect.com/science/article/pii/S2352938517302392 doi:
 515 <https://doi.org/10.1016/j.rsase.2018.06.002>
- 516 Famiglietti, J. S., Ryu, D., Berg, A. A., Rodell, M., & Jackson, T. J. (2008, 01).
 517 Field observations of soil moisture variability across scales. *Water Resources*
 518 *Research*, *44*. doi: <https://doi.org/10.1029/2006wr005804>
- 519 Fick, S. E., & Hijmans, R. J. (2017, 05). Worldclim 2: new 1-km spatial resolu-
 520 tion climate surfaces for global land areas. *International Journal of Climatol-*
 521 *ogy*, *37*, 4302-4315. doi: <https://doi.org/10.1002/joc.5086>
- 522 Ford, T. W., Rapp, A. D., Quiring, S. M., & Blake, J. (2015, 08). Soil mois-
 523 ture–precipitation coupling: observations from the oklahoma mesonet and
 524 underlying physical mechanisms. *Hydrology and Earth System Sciences*, *19*,
 525 3617-3631. doi: <https://doi.org/10.5194/hess-19-3617-2015>
- 526 Franz, T. E., Pokal, S., Gibson, J. P., Zhou, Y., Gholizadeh, H., Tenorio, F. A., ...
 527 Wardlow, B. (2020, 07). The role of topography, soil, and remotely sensed
 528 vegetation condition towards predicting crop yield. *Field Crops Research*, *252*,
 529 107788. doi: <https://doi.org/10.1016/j.fcr.2020.107788>
- 530 Gardner, A. S., Maclean, I. M., & Gaston, K. J. (2019, 05). Climatic predictors of
 531 species distributions neglect biophysiological meaningful variables. *Diversity*
 532 *and Distributions*. doi: <https://10.1111/ddi.12939>
- 533 Garneau, C., Bélair, S., Carrera, M. L., McNairn, H., & Pacheco, A. (2017, 02).
 534 Field-scale spatial variability of soil moisture and l-band brightness tempera-
 535 ture from land surface modeling. *Journal of Hydrometeorology*, *18*, 573-589.
 536 doi: <https://doi.org/10.1175/jhm-d-16-0131.1>
- 537 Green, J. K., Seneviratne, S. I., Berg, A. M., Findell, K. L., Hagemann, S.,
 538 Lawrence, D. M., & Gentine, P. (2019, 01). Large influence of soil mois-
 539 ture on long-term terrestrial carbon uptake. *Nature*, *565*, 476-479. Re-
 540 trieved from <http://www.nature.com/articles/s41586-018-0848-x> doi:
 541 <https://doi.org/10.1038/s41586-018-0848-x>
- 542 Gruber, A., Scanlon, T., van der Schalie, R., Wagner, W., & Dorigo, W. (2019, 05).
 543 Evolution of the esa cci soil moisture climate data records and their underlying
 544 merging methodology. *Earth System Science Data*, *11*, 717-739. Retrieved
 545 2020-10-29, from [https://essd.copernicus.org/articles/11/717/2019/](https://essd.copernicus.org/articles/11/717/2019/essd-11-717-2019.pdf)
 546 essd-11-717-2019.pdf doi: <https://doi.org/10.5194/essd-11-717-2019>
- 547 Gómez, D., Salvador, P., Sanz, J., & Casanova, J. L. (2020, 10). Modelling desert lo-
 548 cust presences using 32-year soil moisture data on a large-scale. *Ecological In-*
 549 *dicators*, *117*, 106655. doi: <https://doi.org/10.1016/j.ecolind.2020.106655>

- 550 He, K. S., Bradley, B. A., Cord, A. F., Rocchini, D., Tuanmu, M.-N., Schmidtlein,
551 S., ... Pettorelli, N. (2015, 10). Will remote sensing shape the next generation
552 of species distribution models? *Remote Sensing in Ecology and Conservation*,
553 *1*, 4-18. doi: <https://doi.org/10.1002/rse2.7>
- 554 Holden, Z. A., Jolly, W. M., Swanson, A., Warren, D. A., Jencso, K., Maneta,
555 M., ... Landguth, E. L. (2019, 09). Topofire: A topographically resolved
556 wildfire danger and drought monitoring system for the conterminous united
557 states. *Bulletin of the American Meteorological Society*, *100*, 1607-1613. doi:
558 <https://doi.org/10.1175/bams-d-18-0178.1>
- 559 Homer, C. G., Dewitz, J., Yang, L., Jin, S., Danielson, P., Xian, G. Z., ... Megown,
560 K. (2011). Completion of the 2011 national land cover database for the conter-
561 minous united states – representing a decade of land cover change information.
562 *Photogrammetric Engineering and Remote Sensing*, *81*, 345-354. Retrieved
563 2019-08-13, from <https://pubs.er.usgs.gov/publication/70146301>
- 564 Hu, Z., Islam, S., & Cheng, Y. (1997, 08). Statistical characterization of remotely
565 sensed soil moisture images. *Remote Sensing of Environment*, *61*, 310-318. doi:
566 [https://doi.org/10.1016/s0034-4257\(97\)89498-9](https://doi.org/10.1016/s0034-4257(97)89498-9)
- 567 Jalilvand, E., Tajrishy, M., Ghazi Zadeh Hashemi, S. A., & Brocca, L. (2019,
568 09). Quantification of irrigation water using remote sensing of soil moisture
569 in a semi-arid region. *Remote Sensing of Environment*, *231*, 111226. doi:
570 [10.1016/j.rse.2019.111226](https://doi.org/10.1016/j.rse.2019.111226)
- 571 Joshi, C., & Mohanty, B. P. (2010, 12). Physical controls of near-surface soil mois-
572 ture across varying spatial scales in an agricultural landscape during smex02.
573 *Water Resources Research*, *46*. doi: <https://doi.org/10.1029/2010wr009152>
- 574 Kerr, Y. H., Waldteufel, P., Richaume, P., Wigneron, J. P., Ferrazzoli, P., Mah-
575 moodi, A., ... Delwart, S. (2012, 05). The smos soil moisture retrieval algo-
576 rithm. *IEEE Transactions on Geoscience and Remote Sensing*, *50*, 1384-1403.
577 doi: <https://doi.org/10.1109/tgrs.2012.2184548>
- 578 Keyel, A. C., Elison Timm, O., Backenson, P. B., Prussing, C., Quinones, S., Mc-
579 Donough, K. A., ... Kramer, L. D. (2019, 06). Seasonal temperatures and hy-
580 drological conditions improve the prediction of west nile virus infection rates in
581 culex mosquitoes and human case counts in new york and connecticut. *PLOS*
582 *ONE*, *14*, e0217854. doi: <https://doi.org/10.1371/journal.pone.0217854>
- 583 Li, B., & Rodell, M. (2013, 03). Spatial variability and its scale dependency of
584 observed and modeled soil moisture over different climate regions. *Hydrology*
585 *and Earth System Sciences*, *17*, 1177-1188. doi: [https://doi.org/10.5194/hess-](https://doi.org/10.5194/hess-17-1177-2013)
586 [17-1177-2013](https://doi.org/10.5194/hess-17-1177-2013)
- 587 Manfreda, S., McCabe, M. F., Fiorentino, M., Rodríguez-Iturbe, I., & Wood, E. F.
588 (2007, 10). Scaling characteristics of spatial patterns of soil moisture from
589 distributed modelling. *Advances in Water Resources*, *30*, 2145-2150. doi:
590 <https://doi.org/10.1016/j.advwatres.2006.07.009>
- 591 Mathys, A., Coops, N. C., & Waring, R. H. (2014, 02). Soil water availability effects
592 on the distribution of 20 tree species in western north america. *Forest Ecology*
593 *and Management*, *313*, 144-152. doi: <https://doi.org/10.1016/j.foreco.2013.11>
594 [.005](https://doi.org/10.1016/j.foreco.2013.11)
- 595 Midgley, G., Hannah, L., Millar, D., Rutherford, M., & Powrie, L. (2002, 11). As-
596 sessing the vulnerability of species richness to anthropogenic climate change
597 in a biodiversity hotspot. *Global Ecology and Biogeography*, *11*, 445-451. doi:
598 <https://doi.org/10.1046/j.1466-822x.2002.00307.x>
- 599 Mohanty, B. P., Famiglietti, J. S., & Skaggs, T. H. (2000, 12). Evolution of soil
600 moisture spatial structure in a mixed vegetation pixel during the southern
601 great plains 1997 (sgp97) hydrology experiment. *Water Resources Research*,
602 *36*, 3675-3686. doi: <https://doi.org/10.1029/2000wr900258>
- 603 Mälicke, M., Hassler, S. K., Blume, T., Weiler, M., & Zehe, E. (2020, 05). Soil
604 moisture: variable in space but redundant in time. *Hydrology and Earth Sys-*

- 605 *tem Sciences*, 24, 2633-2653. doi: 10.5194/hess-24-2633-2020
- 606 O, S., Hou, X., & Orth, R. (2020, 07). Observational evidence of wildfire-promoting
607 soil moisture anomalies. *Scientific Reports*, 10. doi: [https://doi.org/10.1038/
608 s41598-020-67530-4](https://doi.org/10.1038/s41598-020-67530-4)
- 609 Oldak, A., Pachepsky, Y., Jackson, T. J., & Rawls, W. J. (2002, 01). Statistical
610 properties of soil moisture images revisited. *Journal of Hydrology*, 255, 12-24.
611 doi: [https://doi.org/10.1016/s0022-1694\(01\)00507-8](https://doi.org/10.1016/s0022-1694(01)00507-8)
- 612 O'Neill, P., Chan, S., Njoku, E. G., Jackson, T., Bindlish, R., & Chaubell, J. (2019).
613 *Smap enhanced l3 radiometer global daily 9 km ease-grid soil moisture, version
614 3*. Retrieved from <https://doi.org/10.5067/T90W6VRLCBHI>
- 615 Paul, K. I., Polglase, P. J., O'Connell, A. M., Carlyle, J. C., Smethurst, P. J., &
616 Khanna, P. K. (2003, 02). Defining the relation between soil water content and
617 net nitrogen mineralization. *European Journal of Soil Science*, 54, 39-48. doi:
618 10.1046/j.1365-2389.2003.00502.x
- 619 Qiu, J., & Turner, M. G. (2015, 11). Importance of landscape heterogeneity in sus-
620 taining hydrologic ecosystem services in an agricultural watershed. *Ecosphere*,
621 6, art229. doi: <https://doi.org/10.1890/es15-00312.1>
- 622 Rodríguez-Iturbe, I., & Porporato, A. (2007). *Ecohydrology of water-controlled
623 ecosystems: soil moisture and plant dynamics*. Cambridge University Press.
- 624 Rodríguez-Iturbe, I., Vogel, G. K., Rigon, R., Entekhabi, D., Castelli, F., & Rinaldo,
625 A. (1995, 10). On the spatial organization of soil moisture fields. *Geophysical
626 Research Letters*, 22, 2757-2760. doi: <https://doi.org/10.1029/95gl02779>
- 627 Rosenbaum, U., Bogena, H. R., Herbst, M., Huisman, J. A., Peterson, T. J.,
628 Weuthen, A., ... Vereecken, H. (2012, 10). Seasonal and event dynamics
629 of spatial soil moisture patterns at the small catchment scale. *Water Resources
630 Research*, 48. doi: <https://doi.org/10.1029/2011wr011518>
- 631 Rouholahnejad Freund, E., Fan, Y., & Kirchner, J. W. (2020, 04). Global assess-
632 ment of how averaging over spatial heterogeneity in precipitation and poten-
633 tial evapotranspiration affects modeled evapotranspiration rates. *Hydrology
634 and Earth System Sciences*, 24, 1927-1938. doi: [https://doi.org/10.5194/
635 hess-24-1927-2020](https://doi.org/10.5194/hess-24-1927-2020)
- 636 Rouholahnejad Freund, E., & Kirchner, J. W. (2017, 01). A budyko framework
637 for estimating how spatial heterogeneity and lateral moisture redistribution
638 affect average evapotranspiration rates as seen from the atmosphere. *Hydrology
639 and Earth System Sciences*, 21, 217-233. doi: [https://doi.org/10.5194/
640 hess-21-217-2017](https://doi.org/10.5194/hess-21-217-2017)
- 641 Ryu, D., & Famiglietti, J. S. (2005, 12). Characterization of footprint-scale surface
642 soil moisture variability using gaussian and beta distribution functions during
643 the southern great plains 1997 (sgp97) hydrology experiment. *Water Resources
644 Research*, 41. doi: <https://doi.org/10.1029/2004wr003835>
- 645 Ryu, D., & Famiglietti, J. S. (2006). Multi-scale spatial correlation and scaling be-
646 havior of surface soil moisture. *Geophysical Research Letters*, 33. doi: [https://
647 doi.org/10.1029/2006gl025831](https://doi.org/10.1029/2006gl025831)
- 648 Rötzer, K., Montzka, C., & Vereecken, H. (2015, 03). Spatio-temporal variability
649 of global soil moisture products. *Journal of Hydrology*, 522, 187-202. doi:
650 <https://doi.org/10.1016/j.jhydrol.2014.12.038>
- 651 Sadri, S., Pan, M., Wada, Y., Vergopolan, N., Sheffield, J., Famiglietti, J. S., ...
652 Wood, E. (2020, 09). A global near-real-time soil moisture index monitor for
653 food security using integrated smos and smap. *Remote Sensing of Environ-
654 ment*, 246, 111864. doi: <https://doi.org/10.1016/j.rse.2020.111864>
- 655 Simon, J. S., Bragg, A. D., Dirmeyer, P. A., & Chaney, N. W. (2021, 09). Semi-
656 coupling of a field-scale resolving land-surface model and wrf-les to investi-
657 gate the influence of land-surface heterogeneity on cloud development. *Jour-
658 nal of Advances in Modeling Earth Systems*. doi: [https://doi.org/10.1029/
659 2021ms002602](https://doi.org/10.1029/2021ms002602)

- 660 Sivapalan, M., Beven, K., & Wood, E. F. (1987, 12). On hydrologic similarity: 2. a
661 scaled model of storm runoff production. *Water Resources Research*, *23*, 2266-
662 2278. doi: <https://doi.org/10.1029/wr023i012p02266>
- 663 Sylvain, Z. A., Wall, D. H., Cherwin, K. L., Peters, D. P. C., Reichmann, L. G.,
664 & Sala, O. E. (2014, 04). Soil animal responses to moisture availability are
665 largely scale, not ecosystem dependent: insight from a cross-site study. *Global*
666 *Change Biology*, *20*, 2631-2643. doi: <https://doi.org/10.1111/gcb.12522>
- 667 Taufik, M., Torfs, P. J. J. F., Uijlenhoet, R., Jones, P. D., Murdiyarso, D., &
668 Van Lanen, H. A. J. (2017, 05). Amplification of wildfire area burnt by
669 hydrological drought in the humid tropics. *Nature Climate Change*, *7*, 428-431.
670 doi: <https://doi.org/10.1038/nclimate3280>
- 671 Trugman, A. T., Medvigy, D., Mankin, J. S., & Anderegg, W. R. L. (2018, 07). Soil
672 moisture stress as a major driver of carbon cycle uncertainty. *Geophysical Re-*
673 *search Letters*, *45*, 6495-6503. doi: <https://doi.org/10.1029/2018gl078131>
- 674 Vanmarcke, E. (1984). *Random fields : analysis and synthesis*. MIT Press.
- 675 Vereecken, H., Huisman, J., Pachepsky, Y., Montzka, C., van der Kruk, J., Bo-
676 gena, H., ... Vanderborght, J. (2014, 08). On the spatio-temporal dynamics
677 of soil moisture at the field scale. *Journal of Hydrology*, *516*, 76-96. doi:
678 <https://doi.org/10.1016/j.jhydrol.2013.11.061>
- 679 Vergopolan, N., Chaney, N. W., Beck, H. E., Pan, M., Sheffield, J., Chan, S., &
680 Wood, E. F. (2020, 06). Combining hyper-resolution land surface modeling
681 with smap brightness temperatures to obtain 30-m soil moisture estimates.
682 *Remote Sensing of Environment*, *242*, 111740. doi: <https://doi.org/10.1016/j.rse.2020.111740>
- 683
- 684 Vergopolan, N., Chaney, N. W., Pan, M., Sheffield, J., Beck, H. E., Ferguson,
685 C. R., ... Wood, E. F. (2021a). Smap-hydroblocks, a 30m satellite-
686 based soil moisture dataset for the conterminous us. *Scientific Data*, *8*,
687 264. Retrieved from <https://doi.org/10.1038/s41597021010502> doi:
688 [10.1038/s41597021010502](https://doi.org/10.1038/s41597021010502)
- 689 Vergopolan, N., Chaney, N. W., Pan, M., Sheffield, J., Beck, H. E., Ferguson,
690 C. R., ... Wood, E. F. (2021b, 01). Smap-hydroblocks: Hyper-resolution
691 satellite-based soil moisture over the continental united states. *Zen-*
692 *odo*. Retrieved from <https://doi.org/10.5281/zenodo.4441212> doi:
693 <https://doi.org/10.5281/zenodo.4441212>
- 694 Vergopolan, N., & Fisher, J. B. (2016, 10). The impact of deforestation on
695 the hydrological cycle in amazonia as observed from remote sensing. *In-*
696 *ternational Journal of Remote Sensing*, *37*, 5412-5430. Retrieved from
697 <https://doi.org/10.1080/01431161.2016.1232874> doi: [https://doi.org/](https://doi.org/10.1080/01431161.2016.1232874)
698 [10.1080/01431161.2016.1232874](https://doi.org/10.1080/01431161.2016.1232874)
- 699 Vergopolan, N., Xiong, S., Estes, L., Wanders, N., Chaney, N. W., Wood, E. F., ...
700 Sheffield, J. (2021, 04). Field-scale soil moisture bridges the spatial-scale gap
701 between drought monitoring and agricultural yields. *Hydrology and Earth*
702 *System Sciences*. doi: <https://doi.org/10.5194/hess-25-1827-2021>
- 703 Wall, D. H. (2013). *Soil ecology and ecosystem services*. Oxford University Press.
- 704 Wall, D. H., & Virginia, R. A. (1999, 10). Controls on soil biodiversity: insights
705 from extreme environments. *Applied Soil Ecology*, *13*, 137-150. doi: [https://](https://doi.org/10.1016/s0929-1393(99)00029-3)
706 [doi.org/10.1016/s0929-1393\(99\)00029-3](https://doi.org/10.1016/s0929-1393(99)00029-3)
- 707 Wang, S., Zhang, K., van Beek, L. P., Tian, X., & Bogaard, T. A. (2020, 02).
708 Physically-based landslide prediction over a large region: Scaling low-
709 resolution hydrological model results for high-resolution slope stability
710 assessment. *Environmental Modelling & Software*, *124*, 104607. doi:
711 <https://doi.org/10.1016/j.envsoft.2019.104607>
- 712 Western, A. W., & Blöschl, G. (1999, 04). On the spatial scaling of soil mois-
713 ture. *Journal of Hydrology*, *217*, 203-224. doi: [https://doi.org/10.1016/](https://doi.org/10.1016/s0022-1694(98)00232-7)
714 [s0022-1694\(98\)00232-7](https://doi.org/10.1016/s0022-1694(98)00232-7)

- 715 Western, A. W., Grayson, R. B., Blöschl, G., & Wilson, D. J. (2003). Spatial vari-
716 ability of soil moisture and its implications for scaling. In (p. 119–142). CRC
717 Press.
- 718 Youngquist, M. B., & Boone, M. D. (2014, 07). Movement of amphibians
719 through agricultural landscapes: The role of habitat on edge permeabil-
720 ity. *Biological Conservation*, *175*, 148-155. doi: [https://doi.org/10.1016/](https://doi.org/10.1016/j.biocon.2014.04.028)
721 [j.biocon.2014.04.028](https://doi.org/10.1016/j.biocon.2014.04.028)
- 722 Zhang, J., van Westen, C. J., Tanyas, H., Mavrouli, O., Ge, Y., Bajrachary, S., ...
723 Khanal, N. R. (2019, 08). How size and trigger matter: analyzing rainfall- and
724 earthquake-triggered landslide inventories and their causal relation in the koshi
725 river basin, central himalaya. *Natural Hazards and Earth System Sciences*, *19*,
726 1789-1805. doi: <https://doi.org/10.5194/nhess-19-1789-2019>
- 727 Zheng, Y., Brunzell, N. A., Alfieri, J. G., & Niyogi, D. (2021, 01). Impacts of land
728 cover heterogeneity and land surface parameterizations on turbulent character-
729 istics and mesoscale simulations. *Meteorology and Atmospheric Physics*. doi:
730 <https://doi.org/10.1007/s00703-020-00768-9>
- 731 Zhu, Z., Wright, D. B., & Yu, G. (2018, 11). The impact of rainfall space-time struc-
732 ture in flood frequency analysis. *Water Resources Research*, *54*, 8983-8998.
733 doi: <https://doi.org/10.1029/2018wr023550>